molecules

Molecular Polarizability of Sc and C *(Fullerene* and *Graphite)* Clusters

Francisco Torrens

Institut Universitari de Ciència Molecular, Universitat de València, Dr. Moliner 50, E-46100 Burjassot (València), Spain. http://www.uv.es/~icmol. Tel. +34 963 983 182, Fax +34 963 983 156, E-mail Francisco.Torrens@uv.es

Abstract: A method (POLAR) for the calculation of the molecular polarizability $\langle \alpha \rangle$ is presented. It uses the interacting induced dipoles polarization model. As an example, the method is applied to Sc_n and C_n (fullerene and one-shell graphite) model clusters. On varying the number of atoms, the clusters show numbers indicative of particularly polarizable structures. The $\langle \alpha \rangle$ are compared with reference calculations (PAPID). In general, the Sc_n calculated (POLAR) and C_n computed (POLAR and PAPID) are less polarizable than what is inferred from the bulk. However, the Sc_n calculated (PAPID) are more polarizable than what is inferred. Moreover, previous theoretical work yielded the same trend for Si_n, Ge_n and Ga_nAs_m small clusters. The high polarizability of the Sc_n clusters (PAPID) is attributed to arise from dangling bonds at the surface of the cluster.

Keywords: Polarization, polarizability, nanostructure, cluster, fullerene.

Introduction

Benichou *et al*. measured the static electric dipole polarizabilities of lithium clusters made of *n* (*n*=2-22) atoms [1]. The experiment consisted of deflecting a collimated cluster beam through a static inhomogeneous electric field. The strong decrease per atom from Li to Li_3-Li_4 showed that electronic delocalization was reached for very small sizes. Moreover, directly measured polarizabilities were consistent with photoabsorption data. They thus confirmed unambiguously the *missing* optical strength in lithium clusters. Maroulis and Xenides reported highly accurate *ab initio* calculations with specially designed basis sets for Li_4 [2]. The molecule emerged as a particularly soft system, with very anisotroic dipole polarizability and very large second dipole hyperpolarizability. An extensive investigation of basis set and electron correlation effects led to values of $\bar{a}$ = 387.01 and $\boldsymbol{Da}$ = 354.60 a.u. The mean hyperpolarizability was $\bar{\boldsymbol{g}}$ = 2394·10^3 a.u.. They also discussed the computational aspects of the effort in view of the extension of quantumchemical studies to larger lithium clusters. Their values for the mean dipole polarizabilitiy were systematically higher than the recently reported experimental static value (326.6 a.u.) of this important quantity [1].

Fuentealba presented a theoretical study of the static dipole polarizability of carbon clusters C_n with $n \leq$ 8 [3]. They calculated the dipole polarizabilities using density functionals of the hybrid type in combination with the finite field method. They investigated large basis sets in order to obtain reliable results. They showed that the dipole polarizabilities are an important quantity for the identification of clusters with different numbers of atoms and even for the separation of isomers. In particular, they predicted that the jet formed by the two isomers of C_6, cyclic and linear, would split up in the presence of an electric field. Fuentealba and Reyes calculated the dipole polarizability of a series of clusters of the type Li_nH_m using density functional methods [4]. They explained the study of the trends in the mean polarizability and the anisotropy in terms of the interplay between electronic and geometrical effects. They also discussed the changes in the polarizability for different isomers of a given cluster as well as its variations when hydrogen atoms were added to a given cluster. They also calculated a very related quantity, the hardness, in the simple approximation of hardness equal to the energy gap. They discussed their values in terms of the possible stability of the different clusters.

Jackson *et al*. used a first-principles, density-functional-based method to calculate the electric polarizabilities and dipole moments for several low-energy geometries of Si clusters in the size range $10 \leq n$ ≤ 20 [5]. They found that the polarizability per atom is a slowly varying, nonmonotonic function of *n*. Over this size range the polarizability appeared to be correlated most strongly to cluster shape and not with either the dipole moment or the highest occupied—lowest unoccupied molecular-orbital gap. The calculations indicated that the polarizability per atom for Si clusters approaches the bulk limit from above as a function of size. Deng *et al*. calculated the polarizabilities of Si clusters with 9 to 28 atoms using a density functional cluster method [6,7]. They based the atomic geometries on those carefully optimized by energy optimization. The polarizability showed fairly irregular variation with cluster size, but all calculated values were higher than the polarizability of a dielectric sphere with bulk dielectric constant and equivalent volume.

Hohm *et al*. deduced an experimental value of 116.7 ± 1.1 a.u. for the static dipole polarizability of As_4 from the analysis of refractivity measurements in arsenic vapour [8]. This was in close agreement with the theoretical result of 119.5 ± 3.6 a.u., obtained from *ab initio* finite-field many-body perturbation theory and coupled-cluster calculations.

In a previous paper, the following metal clusters and fullerenes were calculated: Sc_n ($1 \leq n \leq 7$ and $n = 12$), C_n ($n = 1, 12, 60, 70$ and 82) and endohedral $Sc@C_{60}$ and $Sc_n@C_{82}$ ($1 \leq n \leq 3$) [9]. In the present paper, the following metal clusters have been calculated: Sc; Sc_2 linear ($D_{\infty h}$); Sc_3 triangle (D_{3h}); Sc_4 in three conformations, square (D_{4h}), rhomb (D_{2h}) and tetrahedron (T_d); Sc_5 triangular bipyramid (D_{3h}); Sc_6 in two conformations, octahedron (O_h) and antiprism (D_{3d}); Sc_7 pentagonal bipyramid (D_{5h}); Sc_{12} icosahedron (I_h); Sc_{17} *(hexagonal close packing*, HCP) and Sc_{74} (HCP). For some clusters, several isomers have been considered. Atom-atom contact distances have been held at 2.945Å. The following fullerene models have been studied: C, C_{12} (I_h), C_{60} (I_h), C_{70} (D_{5h}) and C_{82} (C_2). The following one-shell graphite models have been computed: C_n ($n = 1, 6, 10, 13, 16, 19, 22, 24, 42, 54, 84$ and 96). Atom-atom contact distances have been held at the experimental distance of 1.415Å. In the next section, the description of the electrostatic properties used in this study is presented. Next, the interacting induced dipoles polarization model for the calculation of molecular polarizabilities is presented. Following that, results are presented and discussed. The last section summarizes my conclusions.

Electrostatic properties

Atomic net charges and polarizabilities have been calculated from their s and p contributions [10-14]. The s net charges and polarizabilities have been calculated by the principle of electronegativity equalization [15-18] but applied bond by bond in the molecule [19-22]. The p net charges and polarizabilities have been evaluated with the method of Hückel. The molecule has been brought into its principal inertial coordinate system.

It is well known that p conjugation vanishes for perpendicular structures *(e.g.*, biphenyl). Therefore, the Hückel b parameter can be evaluated, in first approximation, between p_z orbitals twisted from co-planarity by an angle q as $\beta = \beta_o \cos q$, where b_o is equal to the b parameter for benzene [23-33]. Joachim *et al*. [34] evaluated the electronic coupling V_{ab} of the binuclear mixed valence M^{II}-L-M^{III} complex $[(NH_3)_5 Ru\text{-}bipyridyl\text{-}Ru(NH_3)_5]^{5+}$. When a pyridine ring rotates around the ligand axis p-p, $V_{ab}(q)$ was fitted by a $cos^{1.15} q$ function. From this observation, the b function is assumed universal and has the same form as V_{ab} for this complex: $\beta = \beta_o \cos^{1.15} q$.

Interacting induced dipoles polarization model for molecular polarizabilities

The calculation of molecular polarizabilities has been carried out by the interacting induced dipoles polarization model [35-37] that calculates tensor effective anisotropic point polarizabilities by the method of Applequist *et al.* [38-40]. One considers the molecule as being made up of N atoms (represented by i, j, k,…), each of which acts as a point particle located at the nucleus and responds to an electric field only by the induction of a dipole moment, which is a linear function of the local field. If a Cartesian component of the field due to the permanent multipole moments is E_a^i, then the induced moment m_a^i in atom i is:

$$m_a^i = a^i \left(E_a^i + \sum_{j(\neq i)}^{N} T_{ab}^{ij} m_b^j \right) \tag{1}$$

where a^i is the polarizability of atom i and T_{ab}^{ij} is the symmetrical field gradient tensor,

$$T_{ab}^{ij} = 1/e \, \nabla_a^i E_b^j$$

where e is the charge of the proton and the subscripts a, b, c,… stand for the Cartesian components x, y, z. In Equation (1), the expression in parentheses is the total electric field at atom i, consisting of the external field plus the fields of all the other induced dipoles in the molecule.

The set of coupled linear Equations (1) for the induced dipole moments can be expressed conveniently in compact matrix equation form, if one introduces the *3N x 3N* matrices $\bar{\bar{T}}$ and $\bar{\bar{a}}$, with elements T_{ab}^{ij} and a_{ab}^i d^{ij} (d^{ij} being the Kronecker d), respectively. To suppress the restriction in the sum, the diagonal elements T_{ab}^{ij} are defined as zero. Similarly $\bar{E}$ and $\bar{m}$ are *3N x 1* column vectors with elements E_a^i and m_a^i. Equation (1) is thus written in matrix form:

$$\bar{m} = \bar{\bar{a}} \left(\bar{\bar{I}} \, \bar{E} + \bar{\bar{T}} \bar{m} \right) = \bar{\bar{a}} \bar{\bar{I}} \, \bar{E} + \bar{\bar{a}} \bar{\bar{T}} \bar{m}$$

Where $\bar{\bar{I}}$ is the *3N x 3N* -dimensional unit matrix. This matrix equation can be solved for the induced dipoles as

$$\bar{m} = \left(\bar{\bar{I}} - \bar{\bar{a}} \bar{\bar{T}} \right)^{-1} \bar{\bar{a}} \bar{E} = \bar{\bar{A}} \bar{E}$$

Here the symmetrical *many-body* polarizability matrix $\bar{\bar{A}}$ has been introduced:

$$\bar{\bar{A}} = \left(\bar{\bar{I}} - \bar{\bar{a}} \bar{\bar{T}} \right)^{-1} \bar{\bar{a}}$$

The compact matrix equation $\bar{m} = \bar{\bar{A}} \bar{E}$ is equivalent to the N matrix equations:

$$\bar{m}^i = \sum_{j=1}^{N} \bar{\bar{A}}^{ij} \bar{E}^j$$

Let the molecule be in a uniform applied field, so that $\bar{E}^{j} = \bar{E}$ for all j. Then this equation becomes

$$\bar{m}^{i} = \left[\sum_{j=1}^{N} \bar{\bar{A}}^{ij} \right] \bar{E} = \bar{\bar{a}}^{eff,i} \bar{E}$$

The coefficient of $\bar{E}$ in this equation is seen to be an effective polarizability of unit i, $\bar{\bar{a}}^{eff,i}$. The total moment induced in the molecule $\bar{m}^{mol}$ is:

$$\bar{m}^{mol} = \sum_{i=1}^{N} \bar{m}^{i} = \left[\sum_{i=1}^{N} \sum_{j=1}^{N} \bar{\bar{A}}^{ij} \right] \bar{E} = \left[\sum_{i=1}^{N} \bar{\bar{a}}^{eff,i} \right] \bar{E}$$

from which it is seen that the molecular polarizability tensor $\bar{\bar{a}}^{mol}$ is:

$$\bar{\bar{a}}^{mol} = \sum_{i=1}^{N} \sum_{j=1}^{N} \bar{\bar{A}}^{ij} = \sum_{i=1}^{N} \bar{\bar{a}}^{eff,i} \qquad (2)$$

From energetic considerations it is known that $\bar{\bar{a}}$ is a Hermitian matrix [41,42] and must therefore be symmetric if all elements are real.

The significance of a polarizability of $\pm \infty$ is that the molecule is in a state of resonance and absorbs energy from the applied field [43-46]. The following improvements have been implemented in the model:

1. A damping function has been used in the calculation of the symmetrical field gradient tensor in order to prevent the polarizability from going to infinity [47].

2. The interaction between bonded atoms and atoms with a distance lying in an interval defined by $[r^{inf}, r^{sup}]$ has been neglected. The starting values for this interval are $[0,10^{30}]$ and r^{inf} is incremented if resonance conditions are detected.

3. To build up the *many-body* polarizability matrix $\bar{\bar{A}}$ the atomic polarizability tensors given by $\bar{\bar{a}}^{i} = \bar{\bar{a}}^{i}_{s} + \bar{\bar{a}}^{i}_{p}$ have been used instead of the scalar polarizability a^{i}.

A fully operative version of the POLAR program including the whole interacting induced dipoles polarization model has been implemented into the molecular mechanics MM2 program [48] and into the empirical conformational energy program for peptides ECEPP2 [49].

The new versions are called MMID [35,36] and ECEPPID [37]. In both programs, the polarization energy can be now calculated by three options: (1) no polarization, (2) non-interacting induced dipoles polarization model and (3) interacting induced dipoles polarization model.

Calculation results and discussion

The molecular dipole-dipole polarizabilities $<\alpha>$ for the Sc_n clusters are reported in Table 1. Program POLAR gives $<\alpha>$ results that are one third of the corresponding PAPID reference values. This is due to a limitation in the current parametrization of POLAR, that will be improved in a future paper. In particular, the numerical restricted Hartree-Fock (RHF) value for Sc_1 calculated by Stiehler and Hinze (22.317Å^3) is significatively above the POLAR value but of the same order of magnitude as the PAPID one [50].

Table 1. Elementary dipole-dipole polarizabilities for clusters.

Sc_n	$<a> (\text{Å}^3)^a$	$<a>$ ref.^{b}
Sc	5.631	16.893
Sc_2	1.418	13.744
Sc_3	2.103	11.557
Sc_4 D_{4h}	2.111	12.873
Sc_4 D_{2h}	2.461	11.163
Sc_4 T_d	2.657	10.041
Sc_5	3.116	9.690
Sc_6 O_h	3.367	10.330
Sc_6 D_{3d}	3.904	10.330
Sc_7	3.429	9.321
Sc_{12}	3.891	8.724
Sc_{17} h.c.p.	3.590	25.278
Sc_{74} h.c.p.	3.630	23.471

^{a} Average dipole-dipole polarizability (Å^3).

^{b} Reference: calculations carried out with the PAPID program.

The variation of the computed values for the elementary polarizability of Sc_n clusters with the number of atoms is illustrated in Figure 1. The PAPID results for both Sc_6 isomers are nearly equal and so they are superposed. On varying the number of atoms, the clusters show numbers indicative of particularly polarizable structures. Despite the PAPID results for the small clusters tend to the bulk limit, both clusters in the HCP structure comes away from this limit. Thus, both HCP cluster results should be taken with care.
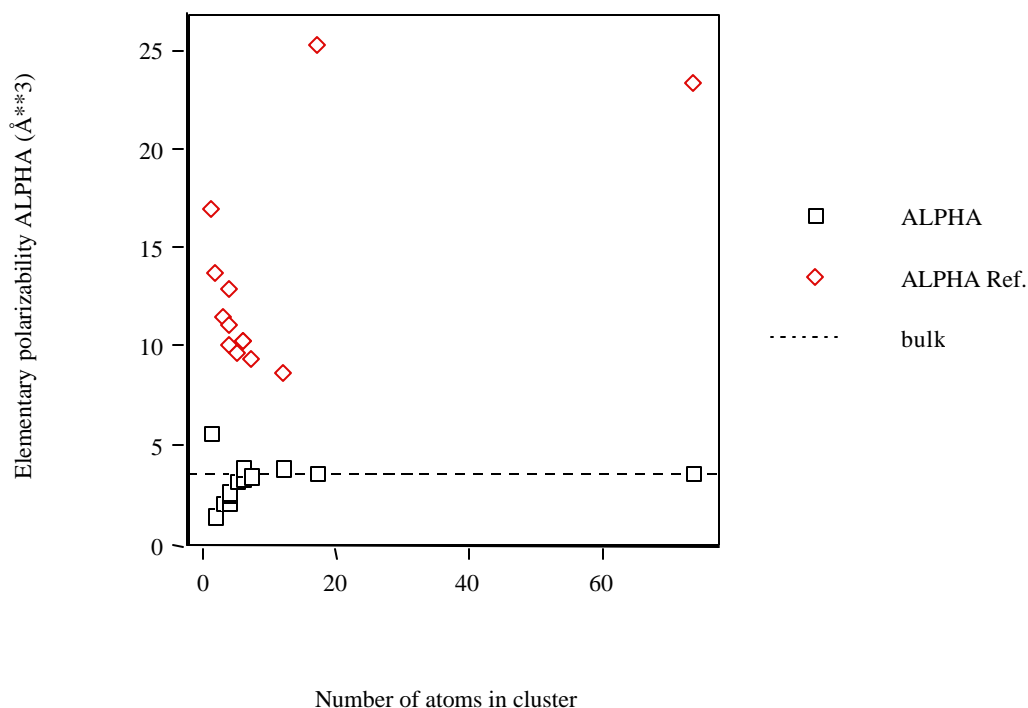
Figure 1. Average atom-atom polarizabilities per atom of Sc$_n$ clusters *vs*. cluster size.
Dotted lines correspond to the bulk polarizabilities.

As a reference, the bulk limit for the polarizability has been included, estimated from the Clausius-Mossotti relationship:

$$a = \frac{3(e-1)v}{4p(e+2)}$$

where v is an elementary volume per atom in the crystalline state and e is the bulk dielectric constant. For metals, e approaches infinite and the dependence of a with e disappears. In this work, the v value used for Sc is 15.0Å^3 per atom, a is calculated as 3.581Å^3 per atom and for C, v=5.3Å^3 and a is obtained as 1.265Å^3.

The polarizability trend for the Sc$_n$ clusters as a function of size is different from what one might have expected. In general, the Sc$_n$ clusters calculated with POLAR are less polarizable than what one might have inferred from the bulk polarizability. Although an exception occurs for Sc$_1$ the trend is clearer after this cluster. Previous experimental work [51] yielded the same trend for Si$_n$, Ga$_n$As$_m$ and Ge$_n$Te$_m$ somewhat larger clusters. However, the Sc$_n$ clusters computed with PAPID are more polarizable than what is inferred

from the bulk, *i.e*., the polarizability of clusters tend to be greater than the bulk limit and approach this limit from above. Moreover, previous theoretical work with density functional theory within the one-electron approximation yielded the same trend for Si_n, Ge_n and Ga_nAs_m small clusters [52]. At present, the origin of this difference is problematic. One might argue that smaller clusters need not behave like those of intermediate size. In addition, the error bars in the experiments are quite large.

The high polarizability of the Sc_n clusters (PAPID) is attributed to dangling bonds at the surface of the cluster. Indeed, most of the atoms within clusters reside on the surface. In fact, these structures are thought more closely related to the high-pressure metallic phases than to the diamond structure [53]. For example, it has been shown that the polarizabilities of alkali clusters significantly exceed the bulk limit and tend to decrease with increasing cluster size [54,55].

The geometries of the C_n fullerene models have been optimized with MMID [35,36]. The polarizabilities $<\alpha>$ for the fullerene models are summarized in Table 2.

Table 2. Elementary dipole-dipole polarizabilities for fullerene models.

C_n **fullerene**	$<\mathbf{a}> (Å^3)^a$	$<\mathbf{a}>$ **ref.**[b]
C	0.588	1.322
C_{12}	0.978	0.722
C_{60}	0.782	0.904
C_{70}	0.781	0.920
C_{82}	0.763	0.911

[a] Average dipole-dipole polarizability ($Å^3$).

[b] Reference: calculations carried out with the PAPID program.

In general, POLAR underestimates $<\alpha>$. In particular, the numerical RHF value for C_1 ($1.783Å^3$) [50] and the density functional theory (DFT) value calculated by Fuentealba ($1.882Å^3$) [3] are significatively above POLAR but on the same order of magnitude as PAPID. For C_{60}, the experimental elementary value measured by Antoine *et al*. ($1.28\pm0.13Å^3$) [56] and the *ab initio* value calculated by Norman *et al*. ($1.430Å^3$) [57] are somewhat greater than those obtained with POLAR and PAPID.

The fullerene models calculated with POLAR and PAPID are, in general, less polarizable than what is inferred from the bulk and approach this limit from below (see Figure 2). Although an exception occurs for C_1 (PAPID) or C_{12} (POLAR) this trend is clearer after this structure.
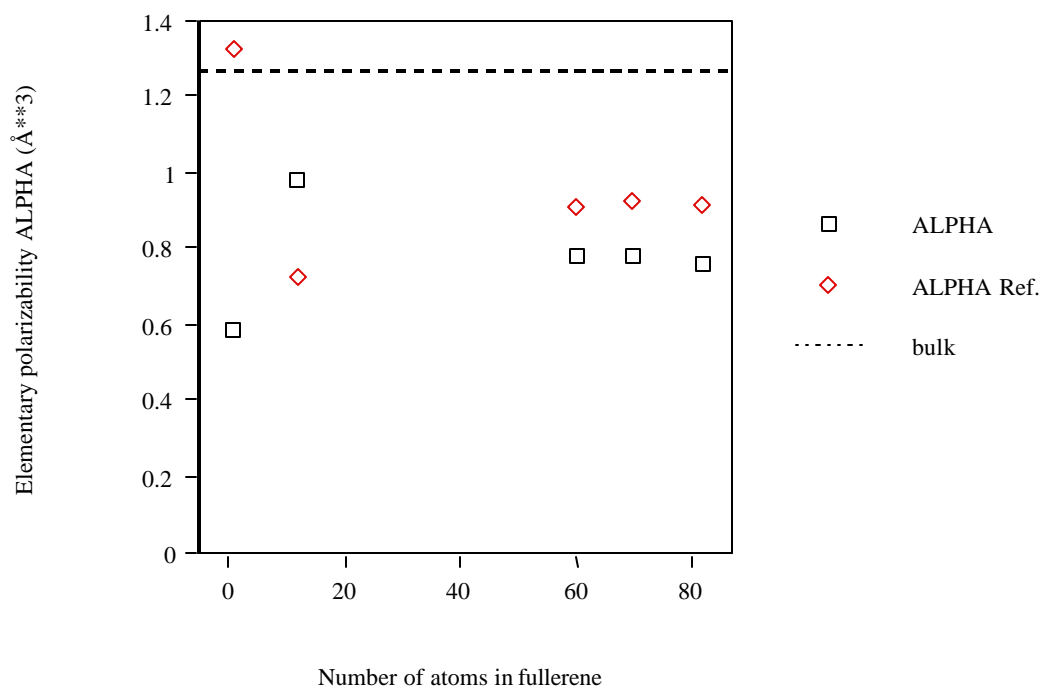
Figure 2. Average atom-atom polarizabilities per atom of fullerene models *vs*. cluster size.

The polarizabilities $<\alpha>$ for the C_n one-shell graphite models are listed in Table 3.

Table 3. Elementary dipole-dipole polarizabilities for one-shell graphite models.

C_n graphite	$<a> (Å^3)^a$	$<a>$ ref.[b]
C	0.588	1.322
C_6	0.746	1.024
C_{10}	0.775	1.067
C_{13}	0.789	1.074
C_{16}	0.795	1.091
C_{19}	0.805	1.109
C_{22}	0.798	1.116
C_{24}	0.796	1.117
C_{42}	0.813	1.185
C_{54}	0.839	1.212
C_{84}	0.851	1.273
C_{96}	0.875	1.293

[a] Average dipole-dipole polarizability ($Å^3$).

[b] Reference: calculations carried out with the PAPID program.

POLAR underestimates <α>. In particular, the DFT value for C_6-cyclic $(1.445Å^3)$ is doubled with respect to POLAR but only somewhat greater than that obtained with PAPID [3]. The graphite models calculated with POLAR and PAPID are, in general, less polarizable than what is inferred from the bulk and approach this limit from below (see Figure 3). Although an exception occurs for C_1 (PAPID) this trend is clearer after this structure.
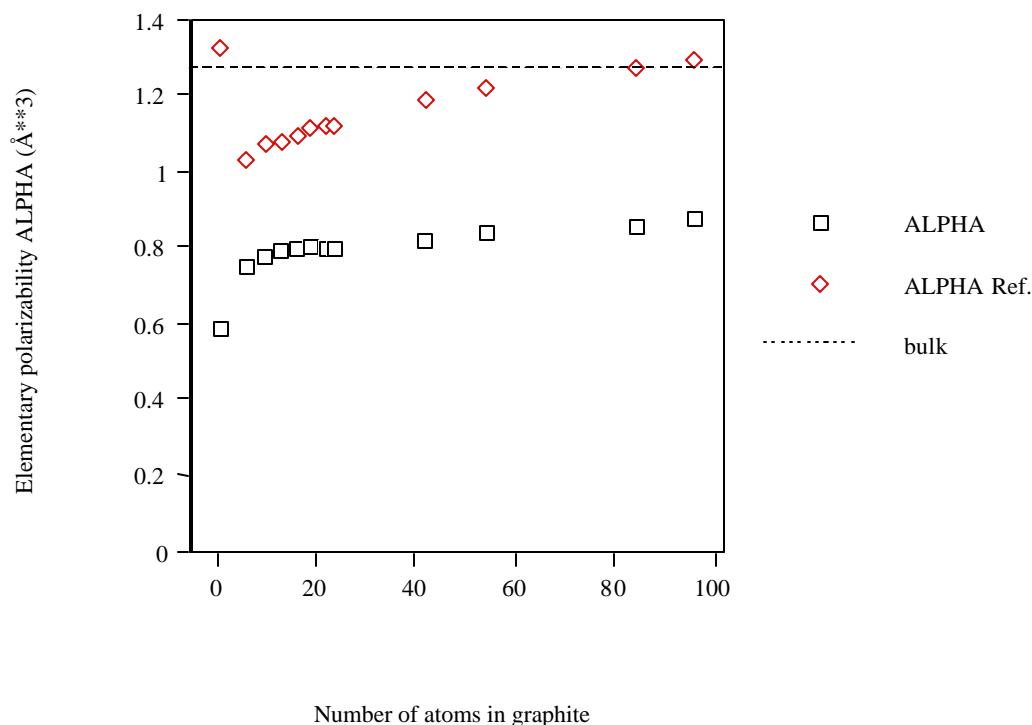

Figure 3. Average atom-atom polarizabilities per atom of one-shell
graphite models *vs*. cluster size.

When comparing Sc_n and C_n, <α> is greater for the three-dimensional (3D) Sc_n clusters than for the two-dimensional C_n clusters. This is due to the 3D character of the *metallic* bond in Sc_n. The <α> is greater for the planar C_n graphite models than for the curved fullerene models due to the weakening of the *p* bonds in the non-planar fullerene structure (see Section Electrostatic properties). For all the clusters in Tables 1 to 3, the mean relative error is -39%. It should be noted that this error improves to -34% if the exception structures are eliminated from the tables. In order to prevent these small figures caused by the algebraic sum, the mean unsigned relative error has been calculated. This error results 44% and decreases to 40% without the exception structures.

Conclusions

A method for the calculation of the molecular dipole-dipole polarizability <α> has been presented and applied to Sc_n and C_n (fullerene and one-shell graphite) model clusters. From the preceding results the following conclusions can be drawn:

1. On varying the number of atoms, the clusters show numbers indicative of particularly polarizable structures. The polarizability also depends on the chosen isomer.

2. The results of the present work clearly indicate that due to the differences between POLAR and PAPID results it may become necessary to recalibrate POLAR. It appears that the results of good quality *ab initio* calculations might be suitable as primary standards for such a calibration. Work is in progress on the recalibration of POLAR.

3. The polarizability trend for the clusters as a function of size is different from what one might have expected. The small Sc_n clusters (POLAR) and the large C_n fullerenes (both POLAR and PAPID) are less polarizable than what one might have inferred from the bulk polarizability. The Sc_n clusters (PAPID) are more polarizable than what is inferred from the bulk. The high polarizability of the Sc_n clusters (PAPID) is attributed to arise from dangling bonds at the surface of the cluster. Recommended elementary polarizability values are 17—22$Å^3$ (Sc_n), 1.8—1.9$Å^3$ (small C_n-*fullerene)*, and 1.3—1.9$Å^3$ (small C_n-*graphite*) and 1.3$Å^3$ (big C_n-*fullerene* and C_n-*graphite)*.

Acknowledgements

References

1. Benichou, E.; Antoine, R.; Rayane, D.; Vezin, B.; Dalby, F. W.; Dugourd, Ph.; Broyer, M.; Ristori, C.; Chandezon, F.; Huber, B. A.; Rocco, J. C.; Blundell, S. A.; Guet, C. Measurement of static electric dipole polarizabilities of lithium clusters: Consistency with measured dynamic polarizabilities. *Phys. Rev. A,* **1999**, *59*, R1-R4.

2. Maroulis, G.; Xenides, D. Enhanced linear and nonlinear polarizabilities for the Li_4 cluster. How satisfactory is the agreement between theory and experiment for the static dipole polarizability?. *J. Phys. Chem. A,* **1999**, *103*, 4590-4593.

3. Fuentealba, P. Static dipole polarizabilities of small neutral carbon clusters C_n *(n=8)*. *Phys. Rev. A,* **1998**, *58*, 4232-4234.

4. Fuentealba, P.; Reyes, O. Density functional study of Li$_n$H$_m$ clusters. Electric dipole polarizabilities. *J. Phys. Chem. A,* **1999**, *103*, 1376-1380.

5. Jackson, K.; Pederson, M.; Wang, C.-Z.; Ho, K.-M. Calculated polarizabilities of intermediate-size Si clusters. *Phys. Rev. A,* **1999**, *59*, 3685-3689.

6. Deng, K.; Yang, J.; Chan, C. T. Calculated polarizabilities of small Si clusters. *Phys. Rev. A,* **2000**, *61*, 025201-1-4.

7. Deng, K.; Yang, J.; Yuan, L.; Zhu, Q. Hybrid density-functional study of Si$_{13}$ clusters. *Phys. Rev. A,* **2000**, *62*, 045201-1-4.

8. Hohm, U.; Goebel, D.; Karamanis, P.; Maroulis, G. Electric dipole polarizability of As$_4$, a challenging problem for both experiment and theory. *J. Phys. Chem. A* **1998**, *102*, 1237-1240.

9. Torrens, F. Molecular polarizability of Sc$_n$, C$_n$, and endohedral Sc$_n$@C$_m$ clusters. *Microelectronic Eng.*, **2000**, *51-52*, 613-626.

10. Torrens, F. Theoretical characterization of iron and manganese porphyrins for catalyzed saturated alkane hydroxylations. *J. Mol. Catal.*, **1997**, *A-119*, 393-403.

11. Torrens, F.; Sánchez-Marín, J.; Nebot-Gil, I. Interacting induced dipoles polarization model for molecular polarizabilities. Application to benzothiazole (A)-benzobisthiazole (B) oligomers: A-B$_{13}$-A. *J. Mol. Struct. (Theochem),* **1998**, *426*, 105-116.

12. Torrens, F.; Sánchez-Marín, J.; Nebot-Gil, I. Torsional effects on the molecular polarizabilities of the benzothiazole (A)-benzobisthiazole (B) oligomer A-B$_{13}$-A. *J. Mol. Graphics,* **1996**, *14*, 245-259.

13. Torrens, F.; Sánchez-Marín, J.; Nebot-Gil, I. Interacting induced dipoles polarization model for molecular polarizabilities. Reference molecules, amino acids and model peptides. *J. Mol. Struct. (Theochem),* **1999**, *463*, 27-39.

14. Torrens, F.; Ortí, E.; Sánchez-Marín, J. Vectorized TOPO program for the theoretical simulation of molecular shape. *J. Chim. Phys. Phys.-Chim. Biol.*, **1991**, *88*, 2435-2441.

15. Mulliken, R. S.; *J. Chem. Phys.*, **1934**, *2*, 782.

16. Huheey, J. E. The electronegativity of groups. *J. Phys. Chem.*, **1965**, *69*, 3284-3291.

17. Sanderson, R. T. An interpretation of bond lengths and classification of bonds. *Science,* **1951**, *114*, 670-672.

18. Bratsch, S. G. Electronegativity equalization with Pauling units. *J. Chem. Educ.*, **1984**, *61*, 588-589.

19. Vogel, A. I. Physical properties and chemical constitution. XXIII. Miscellaneous compounds. Investigation of the so-called coördinate or dative link in esters of oxy acids and in nitro paraffins by molecular refractivity determinations. Atomic, structural, and group parachors and refractivities. *J. Chem. Soc.*, **1948**, 1833-1855.

20. Gresh, N.; Claverie, P.; Pullman, A. Intermolecular interactions: Reproduction of the results of *ab initio* supermolecule computations by an additive procedure. *Int. J. Quantum Chem., Symp.*, **1979**, *13*, 243-253.

21. Applequist, J.; Carl J. R.; Fung, K.-K. An atom dipole interaction model for molecular polarizability. Application to polyatomic molecules and determination of atom polarizabilities. *J. Am. Chem. Soc*., **1972**, *94*, 2952-2960.

22. Applequist, J. Atom charge transfer in molecular polarizabilities. Application of the Olson-Sundberg model to aliphatic and aromatic hydrocarbons. *J. Phys. Chem*., **1993**, *97*, 6016-6023.

23. Lowe, J. P. *Quantum Chemistry;* Academic Press: New York, 1978.

24. Mulliken, R. S. The theory of molecular orbitals. *J. Chim. Phys. Phys.-Chim. Biol*., **1949**, *46*, 497-542.

25. Mulliken, R. S. Magic formula, structure of bond energies, and isovalent hybridization. *J. Phys. Chem*., **1952**, *56*, 295-311.

26. Mulliken, R. S.; Rieke, C. A.; Orloff, D.; Orloff, H. Formulas and numerical tables for overlap integrals. *J. Chem. Phys*., **1949**, *17*, 1248-1267.

27. Streitwieser Jr., A. *Molecular Orbital Theory for Organic Chemists*; John Wiley and Sons: New York, 1961.

28. Mulliken, R. S. Overlap integrals and chemical binding. *J. Am. Chem. Soc*., **1950**, *72*, 4493-4503.

29. Streitwieser Jr., A.; Nair, P. M. Molecular orbital treatment of hyperconjugation. *Tetrahedron,* **1959**, *5*, 149-165.

30. Parr, R. G.; Crawford Jr., B. L. Molecular orbital calculations of vibrational force constants. I. Ethylene *J. Chem. Phys*., **1948**, *16*, 526-532.

31. Dewar, M. J. S. A molecular orbital theory of organic chemistry. II. The structure of mesomeric systems. *J. Am. Chem. Soc*., **1952**, *74*, 3345-3350.

32. Simonetta, M.; Winstein, S. Neighboring carbon and hydrogen. XVI. 1,3-interactions and homoallylic resonance. *J. Am. Chem. Soc*., **1954**, *76*, 18-21.

33. Kreevoy, M. M. A theoretical study of 1,4-dithiadiene by the L.C.A.O.-M.O. method. *J. Am. Chem. Soc*., **1958**, *80*, 5543-5547.

34. Joachim, C.; Treboux, G.; Tang, H. A model conformation flip-flop molecular switch. In: *Molecular Electronics: Science and Technology*, AIP Conference Proceedings No. 262; AIP: New York, 1992; pp.107-117.

35. Torrens, F.; Ruiz-López, M.; Cativiela, C.; García J. I.; Mayoral, J. A. Conformational aspects of some asymmetric Diels-Alder reactions. A molecular mechanics + polarization study. *Tetrahedron,* **1992**, *48*, 5209 -5218.

36. Torrens, F.; Sánchez-Marín, J.; Rivail, J.-L. Interacting induced dipoles polarization in a force field for dipeptide models (glycine derivative). *An. Fís. (Madrid)*, **1994**, *90*, 197-204.

37. Torrens, F. Polarization force fields for peptides implemented in ECEPP2 and MM2. *Mol. Simul*., **2000**, *24*, 391-410.

38. Silberstein, L. *Philos. Mag*., **1917**, *33*, 92.

39. Silberstein, L. *Philos. Mag*., **1917**, *33*, 215.

40. Silberstein, L. *Philos. Mag*., **1917**, *33*, 521.

41. Born, M. *Optik*, (Springer-Verlag, Berlin, 1933), 308.

42. Stuart, H. A. *Die Struktur des freien Moleküls;* Springer-Verlag: Berlin, 1952; p. 363.

43. Kauzmann, W. *Quantum Chemistry;* Academic Press: New York, 1957; p. 568.

44. Mahan, G. D. Davydov splittings in anthracene. *J. Chem. Phys*., **1964**, *41*, 2930-2933.

45. Rhodes, W.; Chase, M. Generalized susceptibility theory. I. Theories of hypochromism. *Rev. Mod. Phys*., **1967**, *39*, 348-356.

46. Philpott, M. R. Dipole Davydov splittings in crystalline anthracene, tetracene, naphthalene, and phenanthrene. *J. Chem. Phys*., **1969**, *50*, 5117-5128.

47. Voisin, C.; Cartier, A.; Rivail, J.-L. Computation of accurate electronic molecular polarizabilities. *J. Phys. Chem*., **1992**, *96*, 7966-7971.

48. Allinger, N. L. Conformational analysis. 130. MM2. A hydrocarbon force field utilizing V_1 and V_2 torsional terms. *J. Am. Chem. Soc*., **1977**, *99*, 8127-8134.

49. Némethy, G.; Pottle, M. S.; Scheraga, H. A. Energy parameters in polypeptides. 9. Updating of geometrical parameters, nonbonded interactions, and hydrogen bond interactions for the naturally occurring amino acids. *J. Phys. Chem*., **1983**, *87*, 1883-1887.

50. Stiehler, J.; Hinze, J. Calculation of static polarizabilities and hyperpolarizabilities for the atoms He through Kr with a numerical RHF method. *J. Phys. B,* **1995**, *28*, 4055-4071.

51. Schäfer, R.; Schlecht, S.; Woenckhaus, J.; Becker, J. A.; Polarizabilities of isolated semiconductor clusters. *Phys. Rev. Lett*., **1996**, *76*, 471-474.

52. Chelikowsky, J. R. The electronic and structural properties of semiconductor clusters and nanostructures. Res. Rep. UMSI 97/132, University of Minnesota Supercomputing Institute, 1997.

53. Jarrold, M. F. Nanosurface chemistry on size-selected silicon clusters. *Science,* **1991**, *252*, 1085-1092.

54. De Heer, W. A. The physics of simple metal clusters: Experimental aspects and simple models. *Rev. Mod. Phys*., **1993**, *65*, 611-675.

55. Brack, M. The physics of simple metal clusters: Self-consistent jellium model and semiclassical approaches. *Rev. Mod. Phys*., **1993**, *65*, 677-732.

56. Antoine, R.; Dugourd, Ph.; Rayane, D.; Benichou, E.; Broyer, M.; Chandezon, F.; Guet, C. Direct measurement of the electric polarizability of isolated C_{60} molecules. *J. Chem. Phys*., **1999**, *110*, 9771-9772.

57. Norman, P.; Luo, Y.; Jonsson, D.; Ågren, H. *Ab initio* calculations of the polarizability and the hyperpolarizability of C_{60}. *J. Chem. Phys*., **1997**, *106*, 8788-8791.

Sample Availability: Not available.